Role of the CMS electromagnetic calorimeter in the hunt for the Higgs boson through the two-gamma decay channel

Marc Dejardin[*†]
Irfu/SPP CEA-Saclay
E-mail: marc.dejardin@cern.ch

The electromagnetic calorimeter of CMS (ECAL) is an hermetic, fine grained and homogeneous calorimeter containing 75848 lead tungstate ($PbWO_4$) crystals, completed by a silicon preshower installed in front of the endcaps. The ECAL sensitivity to decay modes with electromagnetic objects in the final state, such as narrow resonances decaying into two photons, is achieved through its excellent energy resolution and knowledge of the energy scale, as well as its fine granularity. The way this resolution has been optimised, as well as the ECAL performance during 2010-2012, is presented in detail. The ECAL role in the hunt for the Higgs boson, through the 2-gamma decay mode, is discussed.

Calorimetry for High Energy Frontiers - CHEF 2013,
April 22-25, 2013
Paris, France

[*] Speaker.
[†] On behalf of the CMS Collaboration.

1. Introduction

Among the broad physics program of the Compact Muon Solenoid (CMS) experiment[1] at the LHC, the investigation of electroweak symmetry breaking process is one of the major activities. In the Standard Model (SM) of particle physics, the electroweak symmetry is spontaneously broken through the existence of a new scalar field (Higgs field), which materializes itself through a new spin 0 particle called the Higgs boson.

During the design phase of the experiment, in the mid 90's, constraints from LEP measurements, as well as from the direct measurement of the top quark mass[2][3], indicated that if such a boson exists, it should be at relatively low mass ($<$ 170 GeV). The two-photon decay mode ($H \to \gamma\gamma$) is rare (with a branching ratio of only about 0.3 %) but is one of the most sensitive channels in the search for a low mass SM Higgs boson ($m_H < 150$ GeV) and the electromagnetic calorimeter (ECAL) has been designed to optimize our sensitivity in this channel[4].

The experimental signature is a narrow peak in the invariant mass distribution of two isolated photons with high momentum transverse to the beam axis on a large irreducible background from QCD production of two photons. Events where at least one of the photon candidates originates from misidentification of jet fragments contribute to an additional reducible background. The experimental width of the di-photon resonance for a low mass SM Higgs boson is totally dominated by the instrumental invariant mass resolution, dependent on the measurements of the energies of the two photons and the angle between them, as described in equation 1.1 below.

$$\frac{\sigma_{M_{\gamma_1\gamma_2}}}{M_{\gamma_1\gamma_2}} = \frac{1}{2}\left(\frac{\sigma_{E_{\gamma_1}}}{E_{\gamma_1}} \oplus \frac{\sigma_{E_{\gamma_2}}}{E_{\gamma_2}} \oplus \frac{\sigma_{\theta_{\gamma_1\gamma_2}}}{\tan(\frac{\theta_{\gamma_1\gamma_2}}{2})}\right) \tag{1.1}$$

Provided that the correct primary vertex is identified and the photon positions are measured with a precision of about 1cm (easily achievable in the CMS ECAL for the entire range of photon energies considered), the mass resolution is dominated by the energy resolution for the two photons and the precise knowledge of the absolute energy scale.

In this report, the instrumental and operational aspects of the CMS ECAL relevant in the "hunt" for the $H \to \gamma\gamma$ decay are discussed. Particular emphasis is given to in-situ contributions to the energy resolution.

2. The electromagnetic calorimeter of CMS

The CMS ECAL[4] is a compact, hermetic, fine grain and homogeneous calorimeter made of 75848 lead tungstate ($PbWO_4$) scintillating crystals arranged in a quasi-projective geometry and distributed in a barrel region (EB), with pseudorapidity coverage up to $|\eta| = 1.48$, closed by two endcaps (EE) that extend up to $|\eta| = 3$. This design has been driven by the optimization of the detection of photons. For example, the non-projective geometry avoids loss of photons in the small gaps between crystals. Lead tungstate has been chosen for its small radiation length (0.89 cm), which facilitates a compact detector of about 26 radiation lengths located inside the CMS solenoid; its small Molière radius (2.19 cm), allowing a lateral segmentation of 1° in the EB (22x22 mm^2 front face crystals); and its fast response (99 % of the light is collected in 100 ns) compatible with the high interaction rate of the LHC.

The scintillation light of each crystal is readout in EB with two avalanche photodiodes (APDs - 5x5 mm^2 and 75% quantum efficiency (Q.E.)) read in parallel operating at gain 50, and in EE with one vacuum phototriode (VPT - 280 mm^2, 20% Q.E.) operating at gain 10.

The energy resolution of the CMS ECAL can be written as the quadratic sum of 3 contributions:

$$\frac{\sigma_E}{E} = \frac{a}{\sqrt{E}} \oplus \frac{b}{E} \oplus c \ . \tag{2.1}$$

The intrinsic performance of the calorimeter has been extensively tested with electron beams[5]. The stochastic term (a), the electronic noise (b) and the constant term (c) contributions have been shown to match the design requirements: 2.8%, 120 MeV and 0.3% respectively in the barrel for energy reconstruction based on a 3x3 crystal matrix. The constant term is limited by the non-uniformity of the longitudinal response in the crystals.

A preshower detector (ES), based on lead absorber and silicon strip sensors is placed in front of the endcap crystals from $1.65 < |\eta| < 2.6$ to help in π^0/γ separation. The electron/photon separation is limited by the silicon tracker coverage ($|\eta| < 2.5$), which defines the acceptance region for photons in the $H \rightarrow \gamma\gamma$ search.

3. Mitigation of radiation effects

The main effect of radiation (ionising and non-ionising) at the LHC is a wavelength-dependent loss of crystal transparency by the creation of colour centres. This process, saturating and partially recovering in the absence of radiation due to self annealing at room temperature, must be monitored and corrected for, to maintain the stability of the detector. An additional effect of radiation is a decrease to a plateau of the VPT response with accumulated photocathode charge.

A dedicated monitoring system[6] has been developed in order to inject into each crystal laser light at ∼447 nm, close to the emission peak of the scintillation light from $PbWO_4$. It provides a measurement of the response of each crystal every 40 minutes, which is used to correct the energy measurement variation during LHC operation. Inaccuracies associated with this correction affect the intercalibration of the ECAL and results in an increase of the constant term (see below).

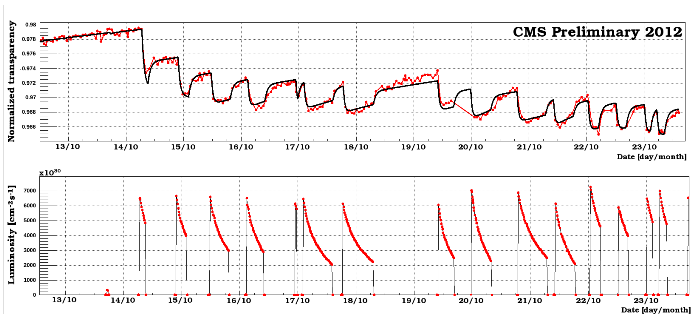

Figure 1: Top: variation of the crystal transparency as measured with the laser monitoring system (red points). The behaviour is well reproduced with a simple dynamical model of 2 colour centres with saturation and recovery (black line). Bottom: Instantaneous luminosity of the LHC delivered in CMS

Fig. 1 shows the transparency variation of one crystal over 3 weeks of data taking in 2012. The behaviour is well reproduced with a simple model of production/recovery/saturation of 2 types of colour centres.

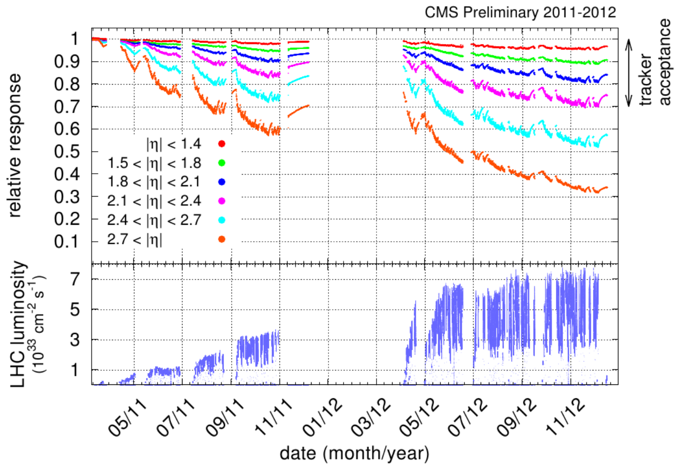

Figure 2: Relative response to laser light (∼447 nm) measured by the ECAL laser monitoring system, averaged over all crystals in bins of pseudorapidity, for 2011 and 2012 data taking periods. The LHC instantaneous luminosity is displayed on the bottom plot.

The measurement of the relative ECAL channel response during 2011 and 2012 data taking periods is illustrated in Fig. 2. The responses are averaged in bins of pseudorapidity (η). In the tracker acceptance region, used for the Higgs boson hunt, the response loss is as high as 30 % at high η values but is limited to 5 % in the central region of the detector (barrel).

According to test beam results[6], the relation between the relative response to scintillation light generated by electromagnetic showers $S(t)/S_0$ and the relative response to laser light $R(t)/R_0$ is a simple power law:

$$\frac{S(t)}{S_0} = \left(\frac{R(t)}{R_0}\right)^{\alpha}, \tag{3.1}$$

where the parameter α is empirically determined and is due to the different paths in the crystals of scintillation and laser light. A few tens of crystals from different production batches and the two manufacturers have been irradiated at test beam facilities and have shown that the spread of α is about 10 % (RMS) for each manufacturer[7] (mean $\alpha = 1.52$ for BTCP[1] crystals and $\alpha = 1.00$ for SIC[2] crystals). With such a spread, using one single value of α per manufacturer can degrade the constant term by 0.1 % in EB and by 1 % in EE. In-situ calibration using, for example, energy-to-momentum (E/p) techniques, allows a better estimation of α in EE of about 1.16.

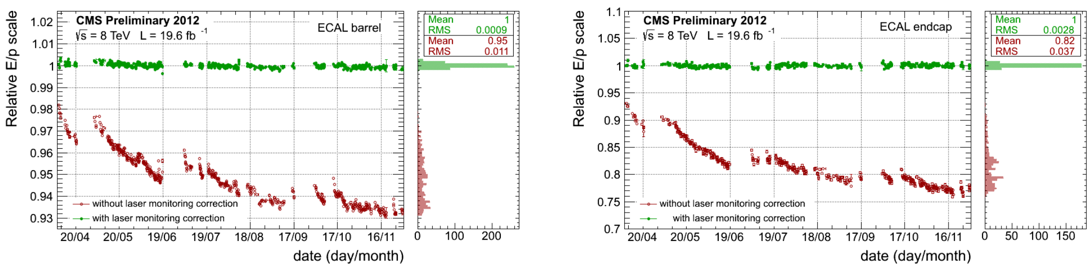

Figure 3: Evolution of the ECAL response using E/p of isolated electrons in EB (left) and EE (right), before (red) and after (green) correction of the response loss as measured by the laser monitoring system.

[1]Bogoroditsk Plant of Technochemical Products, 43, per. Vyazovsky, Bogoroditsk, Tula region, 301801, Russia
[2]Shanghai institute of Ceramics, Chinese Academy of Sciences, 1295 Dingxi road, Shanghai, 200050, P.R. China

Fig. 3 shows the evolution of the ECAL response monitored from the E/p ratio of isolated electrons during the whole 2012 data taking period. An overall stability of 0.11 % was obtained in EB and 0.37 % in EE.

4. Calibration process

The estimation of the electron or photon energy in ECAL involves the collection of the energy deposited by the electromagnetic shower over several crystals. In CMS, the combined action of the strong magnetic field (3.8 T) and the presence of upstream tracker material require the use of dynamic clustering algorithms to recover clusters of energy deposits due to electron bremsstrahlung or photon conversions[8]. The energy of an e/γ candidate is estimated by the following sum over all the crystals (i) belonging to the cluster:

$$E_{e,\gamma} = F_{e,\gamma}(\eta) \cdot \left[G \cdot \sum_i \frac{S_i(t)}{S_0} \cdot C_i \cdot A_i + E_{ES} \right] \tag{4.1}$$

where A_i is the amplitude of the readout signal in ADC counts, C_i is the channel-to-channel intercalibration coefficient, $S_i(t)/S_0$ is the transparency correction at time t as described above and G is the ADC-to-GeV conversion factor which fixes the energy scale of EB and EE separately. The preshower energy E_{ES} is added in the endcap regions. Finally, the sum is corrected for the unclustered energy and for the energy lost upstream of the ECAL by a particle dependent function $F_{e,\gamma}$, which depends mainly on the amount of material in front of ECAL which is η dependent.

4.1 Channel-to-channel intercalibration

The main sources of channel-to-channel response variation are the crystal light yield dispersion due to intrinsic fluctuations in the crystal production process, which is at the level of 15 % and, in EE, the gain and Q.E. spread of the VPTs, which adds about 25 %. All details concerning the calibration of these parameters can be found in [9]. Four types of event are used in the process: minimum bias events, permitting intercalibration in rings of crystals at constant ϕ; π^0 and η resonances; single electrons to compute the E/p ratio; and Z^0 events, which fix the energy scale.

For illustration, Fig. 4 shows the effect of the intercalibration (IC) and the response (LM) correction on the e^+e^- invariant mass of Z^0 candidate events recorded during the 2012 data taking periods.

4.2 Clustering and energy corrections

As mentioned previously, dynamic clustering algorithms are used to form "SuperClusters" in the energy reconstruction to mitigate the impact of the material upstream of ECAL. Corrections take into account unclustered energy due to losses in the tracker material and the effects of the strong magnetic field. These corrections are particle, energy and position dependent due to the different interaction mechanisms of e/γ upstream of ECAL and to the CMS geometry. Corrections have been optimized[10] separately for electrons and photons on Monte Carlo (MC) events with a multivariate analysis (MVA). Input variables include shower shape information on the azimuthal spread of the energy deposit, shower position in ECAL local and CMS global coordinates, and

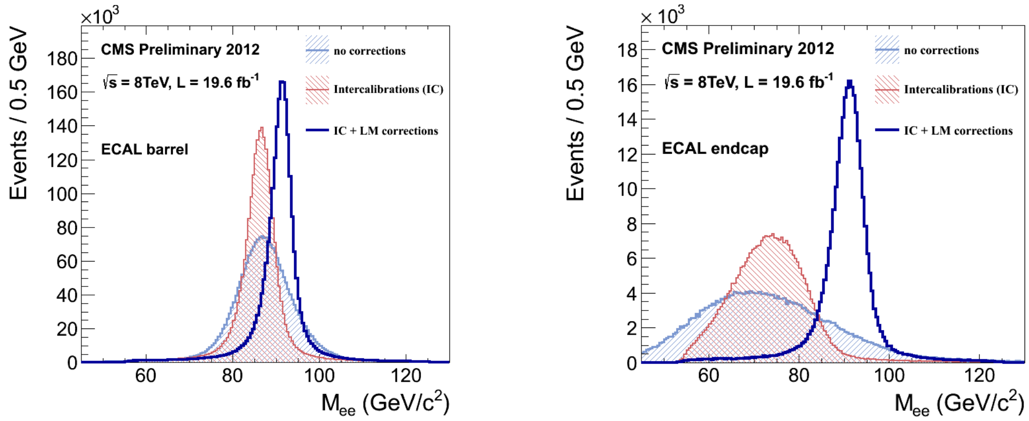

Figure 4: Effect of the intercalibration and transparency corrections on the e^+e^- invariant mass resolution in EB (left) and in EE (right) for Z^0 candidate events.

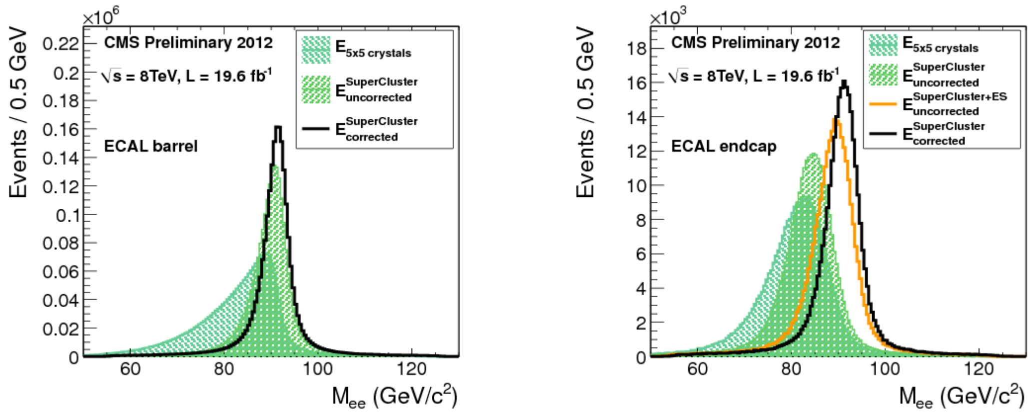

Figure 5: Effect of the dynamic clustering algorithm and energy corrections on the e^+e^- invariant mass resolution in EB (left) and in EE (right) for Z^0 candidate events.

global event variables sensitive to pileup effects. Corrections are sizable at $1 < |\eta| < 2$, where the tracker material thickness is up to two radiation lengths. Due to unavoidable imperfections of the MC model, algorithmic corrections must be tested and tuned on collision data. To this end, the stability of the E/p ratio of electrons is studied as a function of the MVA input variables. MC-driven corrections do not fully compensate for the energy leakage in the inter-crystal gaps, yielding a residual response variation of 0.3-0.5 % RMS.

The improvements obtained through the use of dynamic clustering algorithms and the corrections to the electron energies for the unmeasured energy on the Z^0 candidate events recorded during 2012 data taking periods is shown in Fig. 5.

4.3 Summary of ECAL performance in 2011 and 2012

The performance of the CMS ECAL, in terms of e^+e^- invariant mass resolution, is displayed in Fig. 6 for promptly reconstructed data ($\lesssim$ 48 hours after data taking) using online calibration (grey), after the reprocessing performed during winter 2013 using refined calibration data and algorithms (blue) and for expectations from MC simulation (red). The improvements due to the optimized calibration are clearly visible, especially in the endcap regions ($\eta > 1.5$); the difference between blue and red points illustrates the work remaining in order to understand fully the calorimeter response. This will be addressed in 2 ways: improvement of the description of the

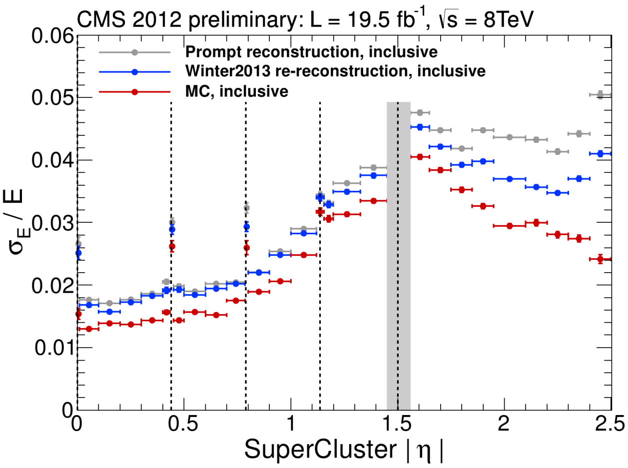

Figure 6: Invariant resolution of e^+e^- for Z^0 candidate events recorded during 2012 data taking periods after prompt reconstruction with online calibration constants (grey), after reprocessing with improved calibrations and algorithms (blue) and expectations from MC simulation (red).

detector in the simulation, especially the amount and distribution of material in front of ECAL, and improvement of the algorithms used in the energy reconstruction. This could eventually result in gains in resolution of ~ 0.5 % and ~ 1 % in EB and EE respectively.

5. Search for a narrow resonance

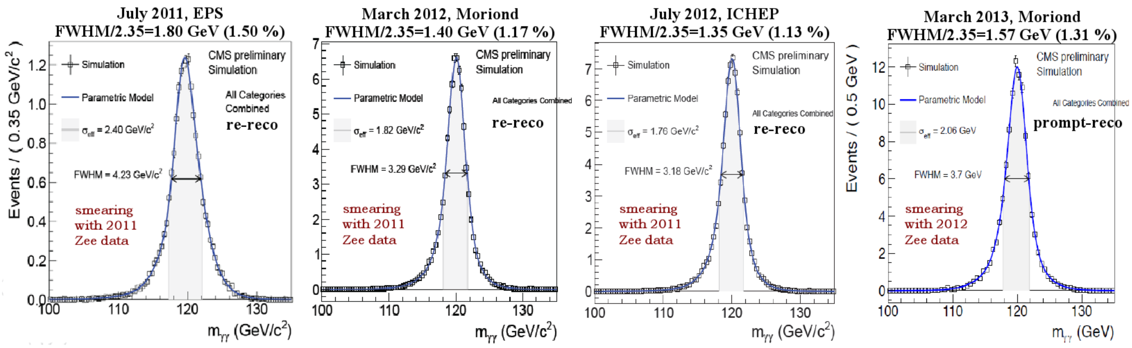

Figure 7: Evolution of the expected invariant mass width for a Higgs boson of 120 GeV decaying to 2 photons. The results presented in Moriond-2013 were obtained with the prompt-reconstruction.

The search for the Higgs boson in the di-photon decay channel is dominated by the energy resolution for the reconstructed photons. In order to precisely simulate the response to photons, the constant term of the energy resolution in the MC is tuned in different regions of ECAL and for the different electromagnetic shower shapes to match the observed resolution in $Z \to ee$ data (Fig. 6), with electrons reconstructed as photons. After this MC tuning using data, the relative invariant mass width of simulated $H \to \gamma\gamma$ events used for the discovery announcement in July 2012[11] (expressed as FWHM/2.35) is 1.13%. This result includes also the additional contribution to the invariant mass resolution coming from the uncertainty of the measured angle between the two photons. However, the latter contribution, given the excellent precision of the ECAL shower position reconstruction, is negligible with respect to the photon energy resolution term in the case of correct assignment of the primary vertex. In Fig. 7 the gradual improvement of the di-photon invariant mass resolution for a 120 GeV Higgs boson is correlated with the main public conferences in 2011 and 2012. As mentioned, the results presented in Moriond in 2013 were not fully optimised; it is expected that the mass resolution will improve further, once the final calibration is applied with data reprocessing.

6. Conclusion and outlook

Thanks to the outstanding performance of the CMS detector and ECAL in particular, in July 2012 the CMS collaboration announced[11] the observation of a new boson at a mass of 125 GeV/c^2 from the analysis of data recorded with an integrated luminosity of 5.1 fb^{-1} at $\sqrt{s} = 7$ TeV and 5.3 fb^{-1} at $\sqrt{s} = 8$ TeV. In March 2013, CMS presented[12] results on the characterization of this new boson with the full luminosity recorded during 2011 and 2012 (5.1 fb^{-1} at $\sqrt{s} = 7$ TeV and 19.6 fb^{-1} at $\sqrt{s} = 8$ TeV). In both cases, the most significant channels used were $H \rightarrow \gamma\gamma$ and $H \rightarrow ZZ \rightarrow 4l$ where the use of the information coming from ECAL was of prime importance.

Going further in the study of the Higgs boson properties and being ready for the "hunt" of new particles will require the ECAL team to reach the ultimate performance of the detector and to be able to maintain this performance during the forthcoming LHC data taking campaigns at $\sqrt{s} =$ 13 TeV starting in 2015. This is our major challenge.

References

[1] S. Chatrchyan et al. The CMS experiment at the CERN LHC. *JINST*, 3:S08004, 2008.

[2] *Proceedings of the 17th Int. Symposium on Lepton-Photon Interactions (LP95)*, page 57, 1995.

[3] R. Raja. Top Quark Mass Results from CDF and D0. *Proceedings of Electroweak interactions and unified theories (Moriond 97)*, pages 77–86, 1997.

[4] CMS collaboration. The Electromagnetic Calorimeter Project: Technical Design Report. *CERN/LHCC*, 97-33, 1997.

[5] P. Adzic et al. Energy resolution of the barrel of the CMS electromagnetic calorimeter. *JINST*, 2:P04004, 2007.

[6] M. Anfreville et al. Laser Monitoring System for the CMS Lead Tungstate Crystal Calorimeter. *Nucl. Instr. and Meth.*, A594:292–320, 2008.

[7] P. Adzic et al. Results of the First Performance Tests of the CMS Electromagnetic Calorimeter. *CMS-Note*, 2005/0020, 2005.

[8] CMS collaboration. CMS Physics Technical Design Report, Volume I. *CERN/LHCC*, 06-021, 2006.

[9] M. Obertino. The challenges involving the calibration of the CMS Electromagnetic Calorimeter at the LHC. *Edition de l'Ecole Polytechnique*, this issue, 2013.

[10] CMS-ECAL collaboration. Electron and photon energy calibration and resolution with the CMS ECAL at $\sqrt{(s)} = 7$ TeV. *Submitted to JINST*, CERN-PH-EP-2013-097, 2013.

[11] S. Chatrchyan et al. Observation of a new boson at a mass of 125 GeV with the CMS experiment at the LHC. *Phys.Lett.*, B716:30–61, 2012.

[12] A. Whitbeck. Measurements of Higgs Boson Properties in CMS. *Presented at Rencontres de Moriond on QCD and High Energy Interactions*, CMS CR-2013/145, 2013.